Received: 15 April 2019 | Accepted: 15 November 2019
DOI: 10.1002/hyp.13659

WILEY

RESEARCH ARTICLE

Establishing irrigation potential of a hillside aquifer in the African highlands

Seifu A. Tilahun[1] | Debebe L. Yilak[1] | Petra Schmitter[2] | Fasikaw A. Zimale[1] | Simon Langan[3] | Jennie Barron[3,4] | Jean-Yves Parlange[5] | Tammo S. Steenhuis[1,5]

[1]Faculty of Civil and Water Resources Engineering, Bahir Dar Institute of Technology, Bahir Dar University, Ethiopia

[2]International Water Management Institute, P.O. 11081, Yangon, Myanmar

[3]International Water Management Institute, HQ, P. O. Box 2075, Colombo, Sri Lanka

[4]Department of Soil and Environment Swedish, University of Agricultural Science, Uppsala, Sweden

[5]Department of Biological and Environmental Engineering, Cornell University, Ithaca, New York, USA

Correspondence
Seifu A. Tilahun, Faculty of Civil and Water Resources Engineering, Bahir Dar Institute of Technology, Bahir Dar University, Bahir Dar, Ethiopia.
Email: satadm86@gmail.com

Tammo S. Steenhuis, Department of Biological and Environmental Engineering, Cornell University, Ithaca, New York, USA.
Email: tss1@cornell.edu

Funding information
CGIAR Research Program on Water, Land and Ecosystems (WLE); Higher Education for Development (HED); Borlaug Leadership Enhancement in Agriculture Program (LEAP); Feed the Future Innovation Lab for Small Scale Irrigation, Grant/Award Number: AID-OAA-A-13-0005; U.S. Agency for International Development

Abstract

Feeding 9 billion people in 2050 will require sustainable development of all water resources, both surface and subsurface. Yet, little is known about the irrigation potential of hillside shallow aquifers in many highland settings in sub-Saharan Africa that are being considered for providing irrigation water during the dry monsoon phase for smallholder farmers. Information on the shallow groundwater being available in space and time on sloping lands might aid in increasing food production in the dry monsoon phase. Therefore, the research objective of this work is to estimate potential groundwater storage as a potential source of irrigation water for hillside aquifers where lateral subsurface flow is dominant. The research was carried out in the Robit Bata experimental watershed in the Lake Tana basin which is typical of many undulating watersheds in the Ethiopian highlands. Farmers have excavated more than 300 hand dug wells for irrigation. We used 42 of these wells to monitor water table fluctuation from April 16, 2014 to December 2015. Precipitation and runoff data were recorded for the same period. The temporal groundwater storage was estimated using two methods: one based on the water balance with rainfall as input and baseflow and evaporative losses leaving the watershed as outputs; the second based on the observed rise and fall of water levels in wells. We found that maximum groundwater storage was at the end of the rain phase in September after which it decreased linearly until the middle of December due to short groundwater retention times. In the remaining part of the dry season period, only wells located close to faults contained water. Thus, without additional water sources, sloping lands can only be used for significant irrigation inputs during the first 3 months out of the 8 months long dry season.

KEYWORDS
Ethiopia, groundwater, highlands, irrigation, Lake Tana, water budget, water storage, water table fluctuation method

1 | INTRODUCTION

As the world's population grows to around 9 billion, demand for agricultural products puts growing pressure on scarce water resources, nowhere more so than in sub-Saharan Africa (SSA). Food security in SSA is closely related to water resources variability (Tucker & Yirgu, 2011). Dry season irrigation is one of the best coping mechanisms for improving food security in a changing climate (Alberti, Cantone, Colombo, Oberto, & La Licata, 2016; Karimov et al., 2013). Other potential mechanisms include drought tolerant crop varieties, planting trees, soil conservation, and changing planting dates (Alemayehu & Bewket, 2017; Bryan, Deressa, Gbetibouo, & Ringler, 2009). However, surface and groundwater resources are limited in most of sub-Saharan Africa (Altchenko & Villholth, 2015; Xie, You, Wielgosz, & Ringler, 2014; You et al., 2011) and are likely to become even more scarce in the future (Gan et al., 2016; Vörösmarty, Ellen, Green, & Revenga, 2005).

Previous studies have explored the viability of small- and large-scale irrigation in sub-Saharan Africa (SSA) through use of surface and groundwater resources. The predictions are highly variable between studies as they are dependent on the calculation of groundwater levels and other water demands (e.g., domestic, livestock, industry and environmental flows) (Pavelic, Smakhtin, Favreau, & Villholth, 2012). According to Xie et al. (2014), by combining surface and groundwater, small-scale irrigable land could increase potentially by 30 million ha in sub-Saharan Africa. Schmitter, Kibret, Lefore, and Barron (2018) estimated that 6.3 million ha in Ethiopia could be irrigated using solar photovoltaic based lifting technologies to extract groundwater up to 25 m depth. Worqlul, Collick, Rossiter, Langan, and Steenhuis (2015) showed that in the Gilgel Abay basin less than 0.1% of the potential irrigable land could be irrigated with the available surface water resources. The greatest weakness in these studies is whether sufficient surface or groundwater is available for planned irrigation (Otoo, Lefore, Schmitter, Barron, & Gebregziabher, 2018).

Groundwater availability for irrigation depends on both the recharge and the loss to stream by baseflow and interflow. In Ethiopia, Kebede (2013) estimated the annual recharge of groundwater based on annual baseflow measurements in the range 0–400 mm/year. Mechal, Wagner, and Birk (2015) using the SWAT model predicted groundwater recharge in the south-eastern Main Ethiopian Rift, from 410 mm/year in the highlands to 25 mm/year on the rift floor. In semi-arid Tigray, Walraevens et al. (2009, 2015) estimated the groundwater storage to vary between 18 and 335 mm/year using MODFLOW. Enku et al. (2016) measured a recharge of 800 mm/year in the sub-humid Fogera plain. Walker et al. (2018) estimated groundwater recharge in the humid highlands from 45 to 814 mm/year depending on the type of method used. Using the appropriate method for determining recharge and groundwater availability is therefore crucial (Guzman, Anibas, Batelaan, Huysmans, & Wyseure, 2016; Walraevens et al., 2009).

Several methods have been used for determining groundwater availability. Theis (1935) developed an analytical solution for finding the transmissivity and specific yield of an aquifer based on the drawdown of a well by pumping. He based his solution on the analogy of Darcy flow in an aquifer with heat flow. Goes (1999), Healy and Cook (2002), and Leiriao, He, Christiansen, Andesen, and Bauer-Gottwein (2009) developed and refined the water table fluctuation (WTF) method in which the seasonal and daily fluctuation of the water table were used to determine the recharge; Brutsaert and Nieber (1977) used the rate of change in river flow during periods without rain to determine the aquifer properties by the change in discharge to short and long time analytical solutions of the aquifer outflow; Pool and Eychaner (1995) performed sophisticated temporal-gravity surveys to measured changes in the differences in gravity between two reference stations on bedrock and six stations at wells. Steenhuis, Jackson, Kung, and Brutaert (1985) used the instantaneous profile method to measure the recharge by measuring simultaneously the change in moisture content and matric potential at several depths within the 2 m soil profile. Finally, Steenhuis and van der Molen (1986) found that the Thornthwaite and Mather (1955) procedure matched the recharge measurements of the instantaneous profile method. This method is based on a water balance (WB) of the rootzone where the actual evaporation is linear function of the potential evaporation at field capacity and zero at wilting point.

From the above list of methods, WTF method is according to Healy and Cook (2002) and Leiriao et al. (2009) the preferred method for determining recharge for unconfined aquifers when specific yield and time series water level data are available. Specific yield needed to convert water table height measurements into water availability can be approximated from soil moisture retention curve (Meinzer, 1923; Veihmeyer & Hendrckson, 1931), from WB analysis (Walton, 1970), or from pumping tests (Barker & Herbert, 1989; Walton, 1970). Finally, the results of Walker et al. (2018) implied that the WTF method should be modified for sloping terrains because the lateral movement of water downslope is significant.

With the increasing interest of agricultural transformation through irrigation both in Ethiopia and Africa, it is important to determine the temporal availability of groundwater storage in highland areas. In the Ethiopian highlands, the land is sloping, and groundwater has relatively short retention times (Alemie et al., 2019, in press). It is important to obtain accurate predictions of the available seasonal groundwater storage both in space and time to support sustainable agricultural intensification through irrigation (Kværnø, Engebretsen, Barneveld, & Deelstra, 2016; Sopocleous, 1991). However, traditional methods such as the WTF method are not suitable without modification. The objective of this study is, therefore, to find effective ways to calculate the spatial and temporal distribution of groundwater storage in sloping shallow aquifers to predict the potential for sustainable groundwater use accurately. The selected Robit Bata watershed in the Lake Tana basin is representative of watersheds in the highlands of Ethiopia where smallholder irrigation takes place to grow chat (a mild narcotic crop) and vegetables.

2 | MATERIALS AND METHODS

2.1 | Description of the study area

The Robit Bata experimental watershed is just under 1,000 ha and is located at the south-eastern edge of Lake Tana, in the headwaters of the Blue Nile, Ethiopia (Figure 1). The area has a sub-humid climate with annual rainfall of 1,450 mm, of which 85% falls from June to September.

Elevation ranges between 1,800 and 2,030 m with slopes up to 44%. Forty-five percent of the area has slopes above 10%. Shallow soils over bedrock can be found in the upper areas while the lower part of the watershed is underlain by an aquifer over basalt bedrock. Massive basalt rock outcrops are visible in riverbeds and occasionally on steeper slopes and quarry sites. Faults can be identified by the Acacia tree growing in lines (Ayenew, Demile, & Wohnlich, 2008). Red soils overlay the basalts of which 31% are Luvisols, 24% Alisols and 19% Nitisols (Figure 1).

Mixed agriculture is the predominant land use accounting for 80% of the area. The livestock graze within the watershed on lands available. Crop production during the rainy season is dominated by cereal crops and to lesser extent legumes. During the dry season small-irrigated plots of Khat, Mango trees and vegetables can be found along the river course and near water bearing faults. Water is

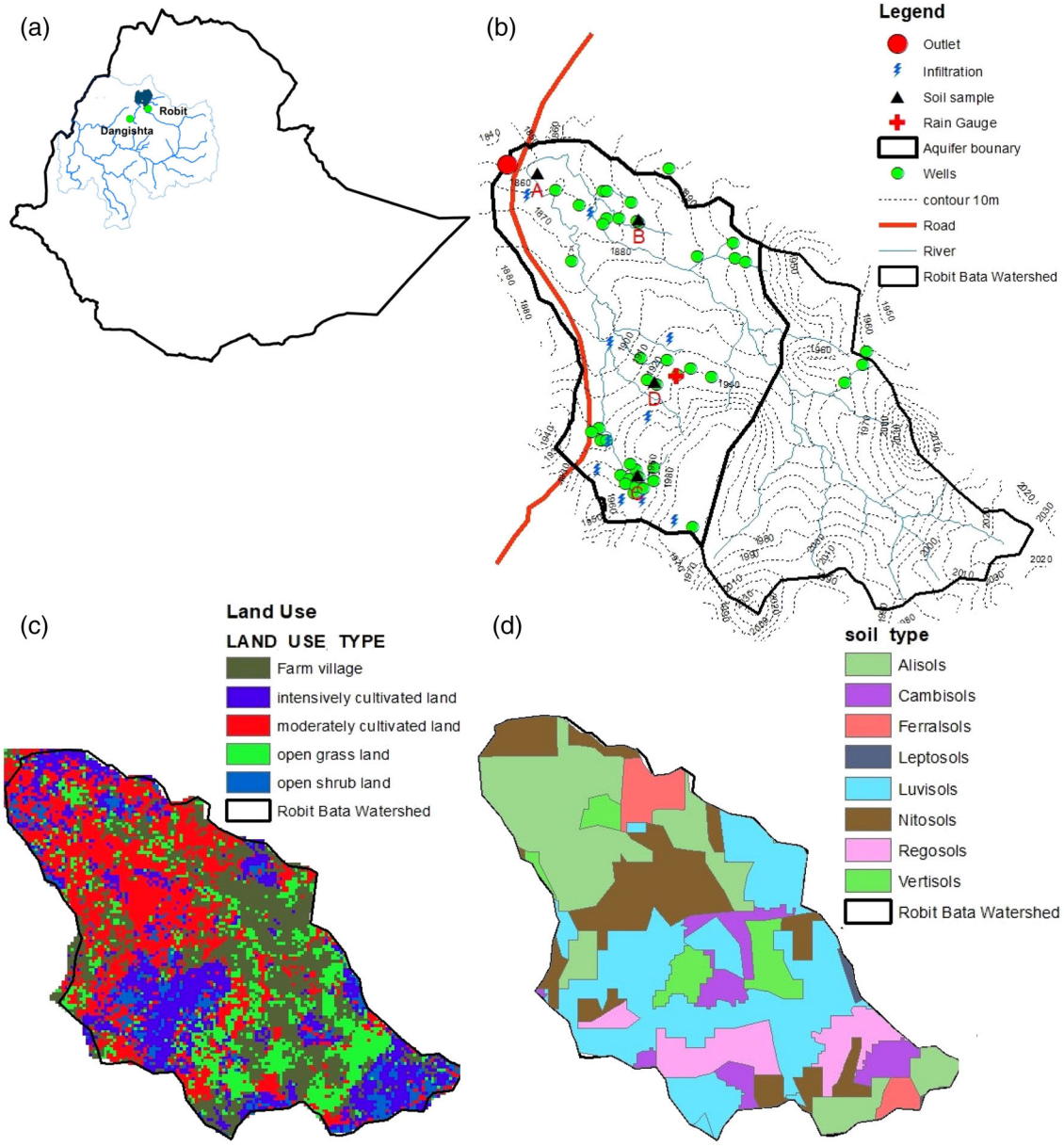

FIGURE 1 Location of Robit Bata watershed. (a) Ethiopia with the Lake Tana Basin in Blue Nile Basin; (b) topographic map with the locations of 40 observation wells (green dots) distributed within Robit Bata watershed, the black line through the watershed divides the lower watershed with an aquifer and the upper watershed with basalt at shallow depth. The red filled circle is the outlet; (c) land use and (d) soil map

abstracted mainly from shallow groundwater during the dry season. Over recent years, smallholder irrigation has expanded in the watershed resulting in an increase in the number of shallow groundwater wells used for irrigation and domestic water supply. The water levels of these wells are on average 4 m depth from the ground surface during the end of rain and up to 8 m depth on average in the dry season. This has led to the drying up of the river in the dry season.

2.2 | Conceptual model for the watershed hillslope aquifers

The watershed has two distinct parts. The eroded upper watershed consists of shallow soils of less than 1 m depth over basalt. Saturation excess runoff prevails when the soil becomes saturated during rainstorms, as infiltration in the subsoil is limited (Tilahun et al., 2013, 2016). The remaining lower half of the watershed has deep soils up to 15 m over basalt containing an aquifer that is the origin of the baseflow and interflow in the rivers. All wells are in the lower half of the watershed (Figure 1).

2.2.1 | Conceptual model for hillslope aquifers

A schematic cross section of the lower part of the watershed with the hillslope aquifer is given in Figure 2. The deep soil (maximum depth 15 m) overlays volcanic basaltic rocks with faults. Due to soil degradation in the highlands, a dense layer with a thickness between 40 and 60 cm is formed below the ploughed rootzone due to leaching of fine soil particles from the surface (Figure 2). This dense layer restricts root growth but has sufficient capacity for rainwater to percolate downward (Tebebu et al., 2015). As a result, the rootzone is often restricted to 10–20 cm (Tebebu et al., 2015). As the ploughed rootzone soil is very permeable and little surface runoff occurs, the percolation is equal to the amount of rainfall minus the water that transpires from the crops and water directly evaporated from the soil surface.

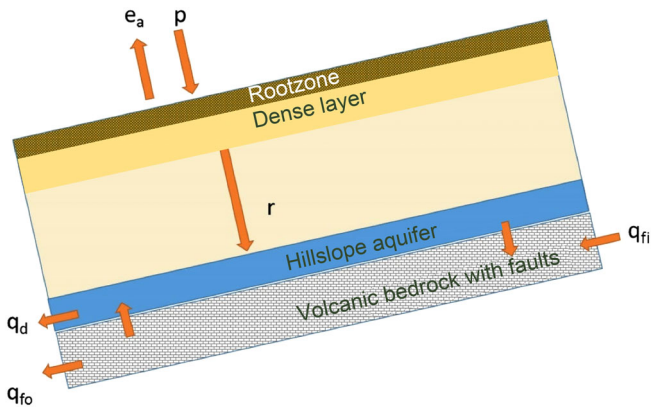

FIGURE 2 Conceptual model of a hillside aquifer with actual evapotranspiration rate, e_a; rainfall rate, p; percolation rate, r, to the hillslope aquifer; lateral flow through the soil matrix, q_d; the rate of later inflow to the faults, q_{fi}; and the rate of lateral outflow from the faults, q_{fo}

The groundwater behaviour in the highlands is very dynamic during the rainy season. When there is both more rainfall (p) than evaporation (e_a) and the soil is above field capacity, excess rain (r) percolates downward so that the soil will be at field capacity. Consequently, a water table builds up in the vadose zone which in hillslope areas flows laterally downward through the soil matrix (q_d) and through the faults (q_f) into the river as interflow (Figure 2). Initially there is more recharge than lateral flow and groundwater builds up. However, as the rainfall decreases the lateral flow is greater than the recharge and the groundwater table decreases. The water table in the vadose zone disappears first at the top of the hill and then gradually moves downhill. As we will see later in the result section, the perched aquifer in the study area has dried up completely by December and the interflow ceases. The river becomes dry and so are most of the wells. Only wells near faults hold water and are located close to Acacia trees which are in line with the faults in the landscape.

2.3 | Calculating shallow groundwater storage in highland areas

We applied two independent methods to calculate the availability of groundwater for irrigation. The first method is based on the WB of the calculated recharge from precipitation and potential evaporation while the second method is a modification of the WTF (Goes, 1999; Healy & Cook, 2002; Leiriao et al., 2009) method using 40 of the 42 monitored shallow that had between 60 and 88 weekly well depth measurements in the period from April 2014 to the December 2015.

2.3.1 | WB method

In the WB method, the groundwater storage can be determined from the mass balance by subtracting the recharge (i.e., the excess water that cannot be stored in the root zone of the portion of the watershed where the aquifer is located) to the groundwater in the area underlain by the aquifer from the baseflow and interflow generated from this aquifer at the outlet, for example,

$$S_{wb} = \int_0^t \left[\frac{A_{aq}}{A_{ws}} r_t - q_t\right] d\tau \quad (1)$$

where S_{wb} is the average aquifer storage expressed as a depth (L) over the whole watershed calculated with the WB method (hence subscript wb). At time t = 0, at the time the groundwater storage starts to fill up, the baseflow starts and S_{wb} = 0, r_t (L/T) is the recharge rate, q_t (L/T) is the baseflow and interflow at the outlet expressed per unit area, A_{aq} (L^2) is the area of the watershed that is underlain by an aquifer, A_{ws} (L^2) is the total watershed area. Thus, in other words the storage in the watershed is equal to the cumulative recharge averaged over the watershed minus the cumulative subsurface outflow. It is assumed that subsurface flow is generated from the lower part of the watershed, and the surface runoff from the upper part of the watershed.

The proportional area was computed with the PED model as explained in the Supplementary material S1 and S2.

Recharge r_t (L/T) to the groundwater (sometimes called potential recharge Walker et al., 2018) was calculated from the widely used Thornthwaite Mather method (Dunne & Leopold, 1978; Steenhuis & van der Molen, 1986; Thornthwaite & Mather, 1955; Tilahun et al., 2013; Walker et al., 2018). The method first calculates the actual evapotranspiration and the change in actual water content of the root zone and then assigns the excess water that cannot be stored in the root zone to either percolation or surface runoff. Actual evapotranspiration was calculated assuming a linearly decrease in evapotranspiration with moisture content from field capacity to wilting point (Steenhuis & van der Molen, 1986). At field capacity, the evapotranspiration is assumed to be equal to the potential evapotranspiration and zero when permanent wilting point is reached. Formally, this can be written as:

$$e_{a_t} = e_{p_t} \quad \text{for } p_t \geq e_{p_t} \tag{2a}$$

$$e_{a_t} = \frac{AW_{t-\Delta t}}{\Delta t}\left[1-\exp\frac{(p_t - e_{p_t})\Delta t}{\text{AWC}}\right] \quad \text{for } p_t < e_{p_t} \tag{2b}$$

where p_t (L/T) is the precipitation on day t, e_p (L/T) is the potential evapotranspiration rate, e_{a_t} (L/T) is the actual evapotranspiration rate, $AW_{t-\Delta t}$ (L) is the available water in the root zone at the previous time step and AWC (L) is the maximum volume of water in root zone (i.e., water holding capacity) per unit area.

The available water in the root zone per unit area on day t, AW_t (L), is either equal to AWC when the rainfall exceeds the storage capacity of the soil or for smaller amounts of rainfall the previous day's moisture content plus the difference of precipitation and evaporation and can be simply written as:

$$AW_t = \min[[AW_{t-\Delta t} + (p_t - e_{a_t})\Delta t], \text{AWC}] \tag{3}$$

For the Robit Bata watershed assuming an average root depth of 20 cm, average field capacity of 0.35 cm^3/cm^3 and average permanent wilting point of 0.2 cm^3/cm^3 resulted in an AWC of 30 mm (Hune, 2016 and Getachew, 2018).

The excess water above the field capacity, r_t (L/T), percolates downward and recharges the groundwater. When the soil is below field capacity, recharge is negligible. Formally, this can be expressed as:

$$r_t = \max[[AW_{t-\Delta t} + (p_t - e_{a_t})\Delta t - AWC], 0] \tag{4}$$

2.3.2 | Modified WTF (mWTF) method

As lateral flow is significant in hillside aquifers, the WTF method, recommended for unconfined aquifers for individual wells without lateral flow, was modified by using the average change in water table height for the aquifer underlying the watershed and including the baseflow at the outlet to account for the lateral flow component. Consequently, groundwater storage at the watershed scale was computed by product of the relative average groundwater water level and the drainable porosity (also called specific yield) of the watershed aquifer and areal proportion of watershed area contributing to the aquifer:

$$S_{\text{mWTF}} = \int_0^t \left[\frac{A_{aq}}{A_{ws}}\eta\left[\bar{h}(\bar{t}) - h_o\right]\right] d\bar{t} \quad \text{for } \bar{h}(\bar{\tau}) \geq h_o \tag{5}$$

where S_{mWTF} (L) is the aquifer storage averaged expressed as a depth of the whole watershed, η (L^3/L^3) specific yield or drainable porosity; $\bar{h}$ (L) average water table height of the aquifer; and h_o (L) is the average groundwater level in the wells (which is 1.7 m as we will see later) when the baseflow ceases to flow (or starts to flow). Groundwater tables below h_o are associated with the faults.

In this method, the specific yield or drainable porosity (η) is a critical variable to convert water table height in amount of groundwater available for irrigation (Delleur, 2010). Enku et al. (2016) found that in the nearby Fogera Plain the soil moisture content decreased linearly with height above the water table and therefore expressed the drainable porosity as:

$$\eta = \frac{\theta_s - \theta_{fc}}{2} \tag{6}$$

with η the drainable porosity, θ_s (L^3/L^3) volumetric soil moisture content at saturation and θ_{fc} (L^3/L^3) the volumetric soil moisture content at field capacity.

2.4 | Hydro-meteorological monitoring in the watershed

2.4.1 | Climate

Five-minute rainfall intensities were recorded in the watershed using one automatic tipping bucket rain gauge with an accuracy of 0.2 mm from May 2014 to September 2015. After September, the automatic rain gauge was not functioning and rainfall to the end of December was collected based on manual readings by farmers. Daily climatic data such as sunshine hours, humidity, wind speed, maximum and minimum temperature to estimate potential evaporation using Penman–Monteith method were obtained from the national meteorological station at the Bahir Dar, located 20 km south of the watershed. The probability of exceedance of rainfall intensity was calculated for the 5-min rainfall intensity and was compared with the steady state infiltration rate.

2.4.2 | Infiltration rates and main runoff mechanisms in the watershed

To confirm that the surface soil has sufficient infiltration capacity when unsaturated, steady state infiltration rates were measured using

30 cm diameter single ring infiltrometer inserted to a depth of 10 cm on 10 locations with different land uses located at different landscape position during rainy season of 2014 (Table 1). The infiltration rates were measured by monitoring the water depth change with time after adding water inside the ring. Measurements were continued until steady state was reached. The median infiltration rate was compared against the exceedance probability of the rainfall intensity. The median is the most meaningful parameter because it represents the central tendency of a spatial distribution of infiltration capacity within the watershed (Bayabil, Tilahun, Collick, Yitaferu, & Steenhuis, 2010; Tilahun et al., 2016).

2.4.3 | Discharge measurement

Manual staff gauges were installed at the watershed outlet at the bridge on the road from Bahir Dar to Gondar (Figure 1). Manual measurements of flow depth and surface velocity were taken from May 1, 2014 to December 31, 2015. Both water level and velocity measurements were taken manually by local data collectors every 20 min during storm events and in addition, at 6:00 a.m. and 6:00 p.m. During days without rain, water flow depths and flow velocities were only monitored at 6:00 a.m. and 6:00 p.m. Some measurements during storm events were affected by local data collectors missing the start of the storm. Surface velocities were determined using the floating method upstream from the outlet of the staff gauges. The time required for the float to reach the staff gauge was recorded. The surface velocities were multiplied by two-third and cross-sectional area at the specific flow depth to compute the mean discharge. A best fit stage-discharge rating curve was developed from all records of depth and discharge. A power-type relationship was fitted to the flow depth and storm discharge (see Supplementary material Figure S1 for stage-discharge rating curves). Storm discharges and non-storm discharges computed from the rating curves within a day were aggregated to obtain the daily discharge which was finally divided by the watershed area to get daily runoff rates in depth units.

2.4.4 | Spatial and temporal groundwater table height measurements and mapping

Weekly groundwater levels were measured in 42 open traditional hand dug wells (called observation wells) using dip meters from middle of April 2014 to end of December 2015 (Figure 1). The average diameter of the wells was 1 m and the depth ranged from 4 m near the streams to 18 m in the upper slopes. In areas where more hand dug wells were found, greater number of observation wells were selected to make sampling more representative.

The average diameter of the wells was 1 m and the depth ranged from 4 m near the streams to 18 m in the upper slopes. In areas where more hand dug wells were found, greater number of wells were selected as observation wells to collect water level data and to make sampling more representative. All these wells were that maintained their water level throughout the year. The average groundwater level above the bedrock was calculated for each day that measurements were taken. Wells not located near faults were dry after January and were abandoned by farmers.

Spatial interpolation of the water table depth from the original ground surface at monthly scale averaging over the 2 years (2014 and 2015) was done over a year using the ordinary kriging option in the Spatial Analyst Tool of ArcGIS. This method was selected because ordinary kriging showed the most acceptable results in groundwater depth interpolation (Nikroo, Kompani-Zare, Sepaskhah, & Shamsi, 2010). The interpolation was done for the part of the watershed where groundwater level data was collected, excluding the upper part of the watershed. The map helps to understand the temporal distribution of the groundwater levels and therefore changes in shallow groundwater storage.

2.4.5 | Determination of specific yield

Soil moisture at saturation and field capacity were determined taking undisturbed soil samples from side wall of the wells at a depth below

TABLE 1 Steady state infiltration rates measured under different land use classes and topographic locations

Topographic location	Land use	Observations on the measurement	Infiltration rate (mm/hr)
Downslope	Eucalyptus tree farm land	Shallow soil depth, subsurface is rocky	350
Downslope	Khat farm land	Measured 24 hr after rainfall	12
Downslope	Mango farm	Measured 24 hr after rainfall	8
Mid-slope	Millet farm land	Measured 48 hr after rainfall	240
Mid-slope	Grassland (protected from free grazing)	Upstream of gully head cut, there is sheet flow during flooding events, measured 48 hr after rainfall	60
Mid-slope	Grassland free grazing	Measured 24 hr after rainfall	8
Upslope	Grassland (protected from free grazing)	Periodically saturated near to stream, measured 24 hr after rainfall	12
Upslope	Grassland	Sloping terrain, measured 24 hr after rainfall	65
Upslope	Millet farm land	Measured 24 hr after rainfall	175
Upslope	Khat farm land	Measured 24 hr after rainfall	200

4 m using a 49 mm diameter and 51 mm high cylindrical core sampler. Four soil samples (A–D, Figure 1) were taken from selected wells along a transect in the watershed: A was taken near to the river outlet, where the basalt bed rock reaches the surface; B was taken upstream representing transported clay loam soil texture mixed with highly weathered rock fragments; C was taken upstream of A near to a tributary stream with a slightly strong weathered rock formation and D taken near to the second mainstream, in a weak highly weathered rock area that is saturated during the wet season. Soil moisture content of the four samples at saturation were determined from the soil porosity using the bulk density samples. Field capacity was determined at 33 kPa (−3.3 m) using the 15 bar plate extractor apparatus of model 1500F2, vessel wt. 39.7 kg and vessel volume 11 L. Median specific yield of 6.5% was estimated using Equation (6) as shown in Table 2. This value was used to estimate the groundwater storage from the groundwater levels data.

3 | RESULTS

3.1 | Rainfall, rainfall intensity and infiltration capacity as function of land use and topography

The Robit Bata watershed received an annual rainfall of 1,486 mm in 2014 and 1,300 mm in 2015 (Figure 3). The average long term from 30 years annual rainfall at the nearest meteorological station of Bahir Dar is 1,400 mm/year. The 5-min rainfall intensity ranged from 3 mm/hr to a maximum of 204 mm/hr (July 30, 2015). The highest rainfall intensities were in August and September.

Steady state infiltration rate for various land uses and topographic positions varied from 8 to 350 mm/hr during the rainy season. Extremely low infiltration rates (below 12 mm/hr) were observed on free grazing lands, farmland covered by khat and mango at the lower reaches of the watershed which were near saturation. Higher values were observed on farmland covered by seasonal crops and tree plantations at both upslope and mid-slope positions (Table 1).

In Figure 4, the 5-min rainfall intensities are compared with the medium infiltration rates of the various slope positions. Downslope, the rainfall intensities exceeded minimum infiltration rate (6–-8 mm/hr) only 20% of the time during the wet season when these soils are near or at saturation. Since in the remaining parts of the watershed the median infiltration rate of 60 mm/hr or above was exceeded by rainfall intensity only 2–2.5% of the time (Figure 4), surface runoff will be minimal, and water will infiltrate in the soil and recharge the perched groundwater table in the upslope soils with basalt at shallow depths or in the perched hillslope aquifer in the lower parts. This lack of surface runoff was also reflected in anecdotal field observation.

TABLE 2 Calculated specific yield (η) with Equation (6) for the four sampled wells in Robit Bata watershed

Soil sample	Bulk density (g/cm^3)	θ_{fc} (%)	θ_s (%)	η (%)
A	1.47	39.4	44.6	2.6
B	1.35	37.9	49.1	5.6
C	1.26	37.5	52.3	7.4
D	1.18	33.6	55.4	10.9
Mean	1.3	37.1	50.4	6.5
Median	1.3	37.7	50.7	6.5

3.2 | Spatial and temporal groundwater levels near the surface

The rise and fall of the monthly average kriged water tables in the northern lower part of the watershed upstream of the outlet is shown in Figure 5. The southern upper part of the watershed has shallow soils of less than 1 m deep that saturates during rainstorms and does not have a water table. The boundary between the upper and lower part (Figure 1) is drawn based on the location of the wells.

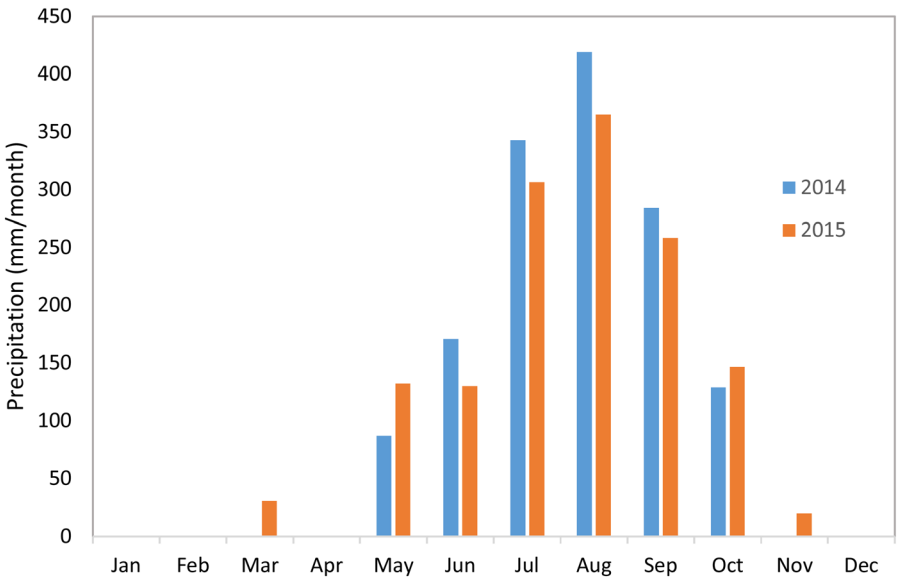

FIGURE 3 Monthly rainfall in Robit Bata watershed

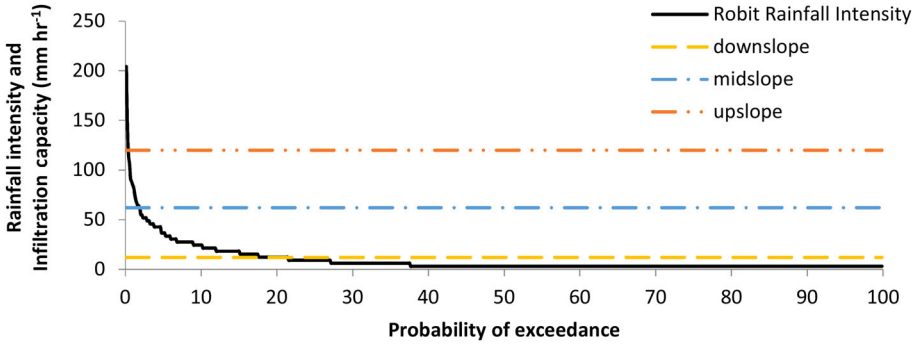

FIGURE 4 Plot of the exceedance probability against rainfall intensities and steady state infiltration capacity in the Robit Bata watershed of the three different landscape position (from Table 2)

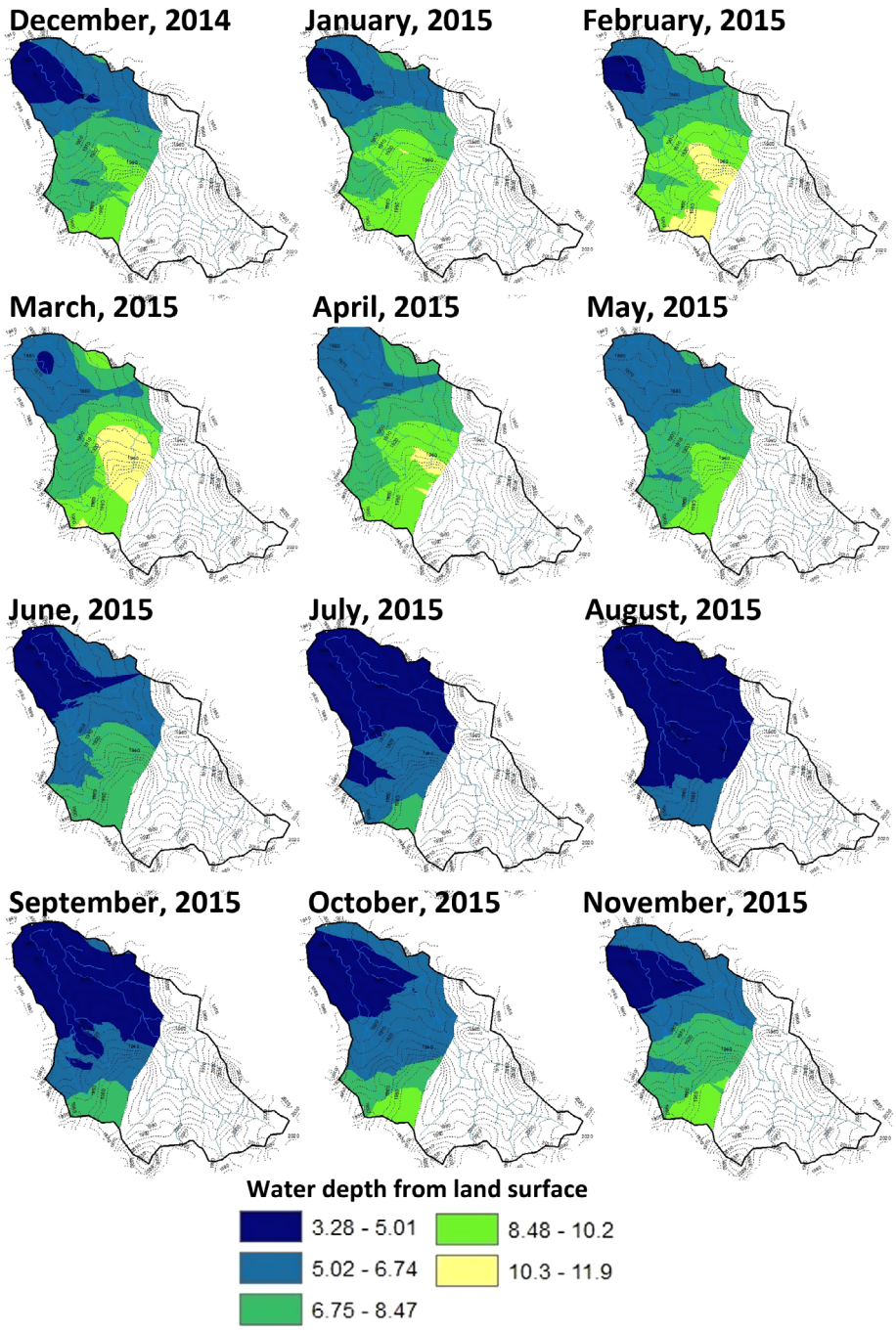

FIGURE 5 Average monthly kriged groundwater depth in Robit Bata watershed from December 2014 to November 2015. Note that only the lower portion of the watershed has deep soils containing a perched water table. The surface elevations and the outlet of the watershed is given in Figure 1

In August, the water table was at its maximum level above the bedrock and ranged between 3 and 5 m from the ground surface over most of the lower part of the watershed (i.e., the dark blue coloured area in Figure 5). In September near the end of the rainy season, the water table decreased slightly but continued to be elevated. Once the rains stopped in October, the water table remained elevated near the outlet but decreased most rapidly farthest away from the watershed outlet (light green areas in Figure 5) and slightly less rapid at intermediate distances. Starting in November, the water table was greater than 7 m below ground surface over half the area of the aquifer (dark and light green areas). From January through May, the water levels were associated with the faults and therefore stayed nearly the same as levels in wells near the boundaries of upper and lower part where the water table is non-existent or very small. In these months, the water table changed only in the centre where the rivers and the fault line are located. Following the first rains in May, the water table started rising mainly along rivers in the centre of the watershed. The increase in water level continued in June when the water level (above the bedrock) increased in the entire aquifer. The height increased (or the depth to the surfaces decreased) further in July and August.

3.3 | Contribution of interflow and baseflow to discharge

Discharge was small in early June but then increased towards the end of the rainy season. The runoff coefficients as ratio of total streamflow to rainfall were computed to understand the temporal distribution of the runoff coefficients. In 2014 and 2015, the runoff coefficients increased with time when the interflow compared to the surface runoff increased. The coefficient reached 0.8 in October 2014 (Figure 6).

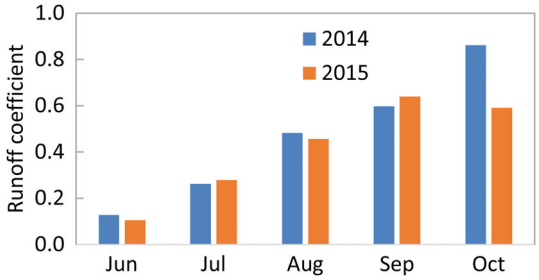

FIGURE 6 Monthly runoff coefficient for the Robit Bata watershed in 2014 and 2015

Both the water table depth in the lower part of the Robit Bata watershed and runoff coefficient increased as the rainy season advances (Figures 5 and 6). This is expected since according to Darcy law the interflow can be calculated as the product of the water table height near the river and the hydraulic gradient. For a hillslope, the hydraulic gradient is nearly equal to the slope of watershed and thus constant. Hence, interflow is directly proportional to the height of the water table for sallow hillslope aquifers. This is consistent with other watersheds in the Ethiopian highlands (Liu et al., 2008; Tilahun et al., 2015).

The contribution of surface runoff and subsurface flow to the hydrograph (both interflow and baseflow) is shown in Figure 7. This separation of the hydrograph was performed with the modified PED model that is described in and Alemie et al. (2019). Details are given in the Supplementary material. The modified PED model assumes that the surface runoff is generated by saturation excess in the upper part of the watershed that has shallow soils over basalt and the subsurface flow in the lower part of the watershed. The portion of the aquifer underlying the watershed (i.e., ratio of A_{aq} to A_{ws}) was 0.52 (see Supplementary material S2). Total estimated annual inter- and baseflow was 477 mm in 2014 and 344 mm in 2015 (Figure 8). The separate components of baseflow and interflow and the portion of the aquifer underlying the watershed were used as input to the WB method to estimate groundwater storage.

3.4 | Calculating shallow perched groundwater storage

3.4.1 | WB method

In the WB method, recharge to the aquifer was estimated using Thornthwaite Mather (Equations (2a)–(4)). The annual estimated recharge in the area overlain by the aquifer was 933 mm in 2014

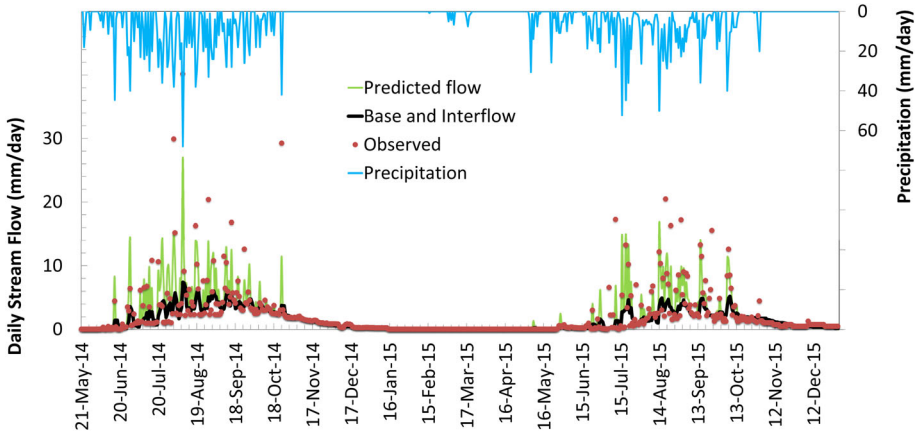

FIGURE 7 Subsurface flow separated from the total streamflow at the outlet of Robit Bata watershed using the PED model

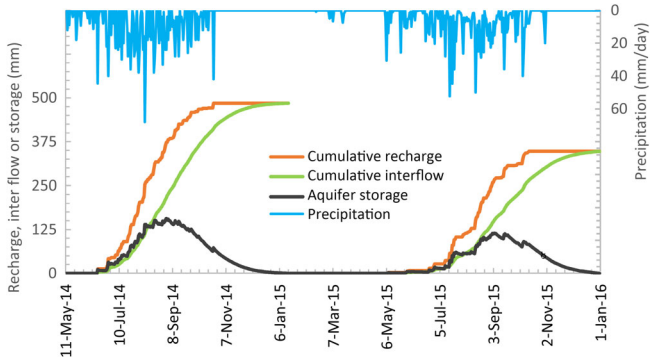

FIGURE 8 Time series plot of rainfall, cumulative recharge (orange), cumulative inter (and baseflow) (green), and groundwater storage (black) all in mm, using Equation (1)

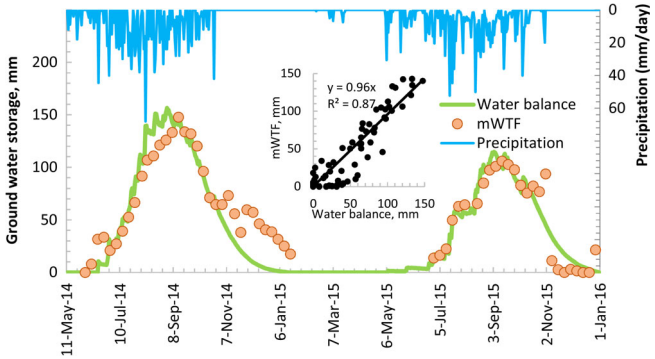

FIGURE 9 Time series plot of rainfall, groundwater storage from water balance (WB) method (Equations (1)–(4)) and modified water table fluctuation (mWTF) method (Equation (5)). The insert compares the water storage of both methods

and 667 mm in 2015. Using PED as explained in the Supplementary material S1 and S2, the portion of the watershed containing the aquifer was estimated as 52%. Using Equation (1), we estimated the aquifer storage as the difference of cumulative recharge and cumulative subsurface discharge at watershed outlet. To adjust the recharge of the aquifer in depth units of the entire watershed, the 52% proportional area of the hillslope aquifer resulted in an estimated recharge of 480 mm in 2014 and 347 mm. The difference between cumulative recharge and cumulative subsurface flow is the storage (green line in Figure 8). The maximum available average groundwater storage over the entire watershed occurred in early September and amounted to 160 mm (or 0.83 hm^3) in 2014 and 115 mm (or 0.60 hm^3) in 2015 (Figure 8).

3.4.2 | mWTF method

The average water table of 40 of 42 wells are shown in Figure S3 in the Supplementary material. Using the mWTF method, the water table data is converted to the perched groundwater storage using the following parameters in Equation (5): the portion of the watershed underlain by the aquifer; the drainable porosity and average height of the water table at time t and the average groundwater level in the wells when the baseflow ceases to flow (or starts to flow). The observed streamflow data showed that the flow begins in 2014 on June 8 and in 2015 on May 28. The average water table was then 1.7 m above the bedrock (Figure S2). This height also corresponds, approximately, when the stream flow ceases in the middle of January. The drainable porosity is given in Table 2 and equals 0.065 cm^3/cm^3. The proportion underlain by the aquifer was similar to that in previous section using the WB method and is equal to 0.52. The resulting storage calculated by the mWTF method is shown in Figure 9 with orange symbols.

The results show that the maximum groundwater storage is reached in the second week of September which is near the end of the rainy season. The maximum storage ranges from 147 mm in 2014 to 106 mm in 2015, a week after the peak storage calculated using the mass balance.

4 | DISCUSSION

4.1 | Interflow explains temporal variations in groundwater storage

The two independent methods to estimate the groundwater storage on sloping deep soils in an experimental watershed in the sub-humid Ethiopian highlands agreed well (Figure 9). The input in the WB method was the daily precipitation, potential evaporation and the baseflow separated hydrograph (Figures 7 and 8). The mWTF method used the average weekly observes groundwater levels (Figure S2) together with the drainable porosity.

The PED model estimated that 52% of the watershed (17% saturated valley bottoms and 35% of the hillslope area) contributes to the shallow aquifer present in the watershed (Table S1). The contribution of the hillslope areas towards the aquifer corresponded well with the Alisols and Nitosols (Figure 1) both with deep soil profiles. Average infiltration rates of 60 mm/hr in the mid-slope positions were exceeded by rainfall intensity only 2–2.5% of the time. Hence, most of the rainfall will be able to infiltrate and move downward over the basaltic rock to the valley bottoms where it reaches the surface and seeps into the stream.

Both models estimated the maximum storage to occur near the end of rainy season and amounted to 125 mm when averaged over the 2 years. The amount stored was only 10% of the rainfall that fell on the watershed and 30% of the recharge in the aquifer portion (Figures 8 and 9).

4.2 | Comparison with literature findings on recharge and storage

Our calculation of recharge and storage is dependent on both the amount of rainfall and the area of the watershed that has deep soils and can store the water. On a watershed basis, the Thornthwaite Mather method calculated that the recharge was 477 mm in 2014 and 344 mm in 2015 when it rained less (Figure 8). When we only consider the portion of the watershed with deep soils in which the water

could infiltrate (i.e., 52% of the watershed) the recharge to the aquifer was 933 mm/year in 2014 and 667 mm/year in 2015. The aquifer storage was approximately one third of the water that was recharged. It was less than the recharge, because groundwater was lost as interflow to the stream during the rain phase. In September, the maximum storage was reached and amounted on average to 125 mm/year over the entire watershed and which is around 250 mm as aquifer storage.

It is difficult to compare the various estimates of storage and recharge in the literature since it is dependent on the amount of rainfall and the watershed characteristics. Kebede (2013) estimated an average of 800 mm of permanent storage and a recharge ranging from 0 to 400 mm/year in all of Ethiopia and 180 mm/year in the Blue Nile basin (chap. 7, Kebede, 2013). Other recharge estimates given in the introduction generally are in the range given by Kebede (2013). Our watershed recharge value is at the high end of this range. The only recharge value that is much greater than the others is by Enku et al. (2016) who measured a recharge and storage of 800 mm/year in the nearby Fogera Plain which is entirely underlain by an aquifer and has a slope less than 0.1%. Thus, the recharge value in Enku et al. (2016) agree with the average recharge value on the aquifer in Robit Bata of 800 mm/year on the average over the 2 years. The storage in the Fogera Plain is much greater because the interflow is negligible, and the water can be stored in the entire watershed.

The shallow hillside aquifers behave differently than the major aquifers in Africa. While pumping at rate greater than the recharge for the major aquifers will cause a permanent and unsustainable decline in the groundwater (Tilman, Cassman, Matson, Naylor, & Polasky, 2002) such as experienced in China, India and Middle East to North America, this is not case for hillside aquifers with travel times shorter than the dry monsoon phase. Over irrigation of crops might actually help keep the water longer in the vadose zone and thereby possibly extend the irrigation season. In addition, investing in water saving agriculture will not result in more water available for the crop of the farmer later in the season, because the velocity of the drying front is independent of the height of the water table. The benefit of water savings agriculture is for the downstream water users because it will increase the downstream baseflow. Finally, mitigating climate change by storing more water in the season so that the aquifer is recharged as proposed by Alberti et al. (2016) and Karimov et al. (2013) will not be feasible.

4.3 | Importance of temporal shallow groundwater storage for small-scale irrigation

Detailed understanding of spatial and temporal variation of groundwater availability and levels can support smallholder irrigation initiatives in designing and implementing feasible smallholder solutions. We found that for a sloping watershed typical for the Ethiopia highlands that shallow groundwater levels peaked throughout the valley bottoms and mid-slopes in September reaching on average 3–5 m below the surface depending on their location (Figure 5). From October to December, groundwater levels rapidly dropped in the up- and mid-slope areas as interflow receded. In January wells in the mid-slope areas started to dry up which is approximately 100–120 days after the rainy season had finished. As a result, the average groundwater depth in the majority of the watershed drops below 10 m in the mid-slope and below 7 m in the lowland with the exception of wells located near the faults.

Understanding the temporal variability of the groundwater storage and the spatial variability of water levels provides useful information for smallholder farmers in selecting suitable dry season crops and lifting technologies. Especially, farmers who have newly made the transition from rainfed systems to intensified irrigated agriculture in the dry season could considerably reduce risks of crop failure through information on available shallow groundwater. The sloping upland areas will have limited to no shallow ground water available from December to January onwards in the dry monsoon phase. Hence, dry season irrigation will be possible only from October to December/January which translates in one high value crop season with a cultivation period of approximately 80–100 days such as onion, lettuce, carrots and beans (Allen, Pereira, Raes, & Smith, 1998). A second crop (e.g., chilli or tomato) or a perennial crop (e.g., khat) will be possible only on a small part in the valley bottom where the groundwater in the faults can be accessed. All of this will contribute to increased food security and potentially introduce new lines of income to diversity agricultural livelihoods.

5 | CONCLUSION

The groundwater availability in a sloping watershed in the Ethiopian highlands was evaluated with two independent methods. The two methods agreed well and indicated that the recharge to the portion of the watershed with aquifer was significant (up to 500 mm/year when averaged over the watershed and 933 mm in the deep soil portion). However, subsurface outflow rates were high as well due the slope of the aquifer and most of the water that was recharged during the rain phase was lost as interflow and baseflow within a first 3-month period of the dry phase. Since interflow amount depend on the slope, the smaller the slope the longer the ground water will be available. The practical significance is that hillside aquifers in deep soils can only be used for irrigating crops in a 3- to 4-month period after the monsoonal rain season ends. The only limited water available during the remainder of the dry phase is from wells in valley bottoms associated with geological faults.

Since donors and governmental agencies consider extending smallholder groundwater irrigation vital for increase food production, our results are directly relevant to planning of smallholder irrigation on rainfed agricultural lands in sub-Saharan Africa. Many of these potential areas are hillside/sloping lands with challenging access to surface water, often implying expensive uphill pumping. Our results suggest that for planning purpose lateral subsurface flow on even the slightly sloping lands should be considered in estimating the quantity of water that can be stored in shallow groundwater for small-scale irrigation interventions. By simply considering the recharge only and ignoring the lateral movement of water, irrigation potential will be unrealistic in actual practice. Moreover, practices such as recharging additional water during the recharge period as advocated for level lands, do not apply to the shallow hillslope aquifers.

Future research in specifying the water availability and water yields in hillside might focus especially in answering two issues that this study was not able to address: First of all, the origin of the water in the wells near faults from January through the beginning of the rain phase should be investigated. We expect that this water comes from the unsaturated vadose zone, percolating slowly downward as unsaturated flow and then flows sideways over sloping bedrock where it collects in the soil near the faults. Second, the effect of slope on water availability should be examined further. We expect that when the slope becomes smaller, the groundwater will last longer after the rain phase ends because the velocity of the water is slower because the hydraulic gradient becomes smaller. In the nearby Fogera Plain with a slope of 0.1%, the water is available year around. It would be helpful for planning purposes to know the maximum slope and at the type of soils that will assure year around availability of groundwater.

ACKNOWLEDGEMENTS

This publication was made partly possible through funds provided U.S. Agency for International Development several programs: through Feed the Future Innovation Lab for Small Scale Irrigation (contract no. AID-OAA-A-13-0005), Borlaug Leadership Enhancement in Agriculture Program (LEAP), and Higher Education for Development (HED). Additional support was received of the CGIAR Research Program on Water, Land and Ecosystems (WLE) supported by CGIAR Fund Donors. The research was implemented under a collaborative partnership between Cornell University, IWMI and Bahir Dar University. The opinions expressed herein are those of the authors and do not necessarily reflect the views of the sponsoring agencies.

DATA AVAILABILITY STATEMENT

The data that support the findings are available in the supplementary material.

ORCID

Seifu A. Tilahun https://orcid.org/0000-0002-5219-4527
Petra Schmitter https://orcid.org/0000-0002-3826-7224
Tammo S. Steenhuis https://orcid.org/0000-0003-0508-9350

REFERENCES

Alberti, L., Cantone, M., Colombo, L., Oberto, G., & La Licata, I. (2016). Assessment of aquifer groundwater storage for the mitigation of climate change effects. *Rendiconti Online Societa Geologica Italiana*, *39*, 89–92. https://doi.org/10.3301/ROL.2016.54

Alemayehu, A., & Bewket, W. (2017). Smallholder farmers' coping and adaptation strategies to climate change and variability in the central highlands of Ethiopia. *Local Environment*, *22*(7), 825–839. https://doi.org/10.1080/13549839.2017.1290058

Alemie, T. C. Tilahun, S. A., Ochoa-Tocachi, B. F. Schmitter, P., Buytaert, W., Parlange, J.-Y., & Steenhuis, T. S. (2019). *Predicting shallow groundwater tables for sloping highland aquifers*. Submitted for publication. Water Resources Research. In Press.

Allen, R. G., Pereira, L. S., Raes, D., & Smith, M. (1998). *Crop evapotranspiration-guidelines for computing crop water requirements—FAO irrigation and drainage paper 56* (p. 300). Rome: Food and Agriculture Organization of the United Nations.

Altchenko, Y., & Villholth, K. G. (2015). Mapping irrigation potential from renewable groundwater in Africa—A quantitative hydrological approach. *Hydrology and Earth System Sciences*, *19*, 1055–1067. https://doi.org/10.5194/hess-19-1055-2015

Ayenew, T., Demile, M., & Wohnlich, S. (2008). Hydrogeological framework and occurrence of groundwater in the Ethiopian aquifers. *Journal of African Earth Sciences*, *52*, 97–113. https://doi.org/10.1016/j.jafrearsci.2008.06.006

Barker, J., & Herbert, R. (1989). Nomograms for the analysis of recovery tests on large-diameter wells. *Quarterly Journal of Engineering Geology and Hydrogeology*, *22*, 151–158. https://doi.org/10.1144/GSL.QJEG.1989.022.02.07

Bayabil, H. K., Tilahun, S. A., Collick, A. S., Yitaferu, B., & Steenhuis, T. S. (2010). Are runoff processes ecologically or topographically driven in the (sub) humid Ethiopian highlands? The case of the Maybar watershed. *Ecohydrology*, *3*, 457–466. https://doi.org/10.1002/eco.170

Brutsaert, W., & Nieber, J. L. (1977). Regionalized drought flow hydrographs from a mature glaciated plateau. *Water Resources Research*, *13*(3), 637–643. https://doi.org/10.1029/WR013i003p00637

Bryan, E., Deressa, T. T., Gbetibouo, G. A., & Ringler, C. (2009). Adaptation to climate change in Ethiopia and South Africa: Options and constraints. *Environmental Science and Policy*, *12*, 413–426. https://doi.org/10.1016/j.envsci.2008.11.002

Delleur, J. W. (2010). *The handbook of groundwater engineering* (p. 1320). Boca Rouge: CRC Press.

Dunne, T., & Leopold, L. B. (1978). *Water in environmental planning* (p. 818). New York: Freeman.

Enku, T., Melesse, A. M., Ayana, E. K., Tilahun, S. A., Abate, M., & Steenhuis, T. S. (2016). Groundwater evaporation and recharge for a floodplain in a sub humid monsoon climate in Ethiopia. *Land Degradation & Development*, *28*, 1831–1841. https://doi.org/10.1002/Ldr.2650

Gan, T. Y., Ito, M., Hülsmann, S., Qin, X., Lu, X. X., Liong, S. Y., … Koivusalo, H. (2016). Possible climate change/variability and human impacts, vulnerability of drought-prone regions, water resources and capacity building for Africa. *Hydrological Sciences Journal*, 1–18. https://doi.org/10.1080/02626667.2015.1057143

Getachew, T. (2018). *Development of crop coefficient and evaluation of partial nutrient balance for garlic (*Allium sativum*) and inter cropped Napier grass under dry period irrigation in Robit Bata watershed*. (MS thesis). Bahir Dar, Ethiopia: Bahir Dar Institute of Technology-Bahir Dar University.

Goes, B. (1999). Estimate of shallow groundwater storage in the Hadejia–Nguru wetlands, semi-arid northeastern Nigeria. *Hydrogeology Journal*, *7*, 294–304. https://doi.org/10.1007/s100400050203

Guzman, P., Anibas, C., Batelaan, O., Huysmans, M., & Wyseure, G. (2016). Hydrological connectivity of alluvial Andean valleys: A groundwater/surface-water interaction case study in Ecuador. *Hydrogeology Journal*, *24*, 1–15. https://doi.org/10.1007/s10040-015-1361-z

Healy, R. W., & Cook, P. G. (2002). Using groundwater levels to estimate storage. *Hydrogeology Journal*, *10*, 91–109. https://doi.org/10.1007/s10040-001-0178-0

Hune, M. G. (2016). *Evaluation of irrigation scheduling strategies on partial nutrient balance for tomato production during the dry season at Robit Bata watershed*. (MS Thesis). Bahir Dar, Ethiopia: Bahir Dar Institute of Technology-Bahir Dar University.

Karimov, A., Smakhtin, V., Mavlonov, A., Borisov, V., Gracheva, I., Miryusupov, F., … Abdurahmanov, B. (2013). Managed aquifer recharge: The solution for water shortages in the fergana valley. *IWMI Research Report*, *151*, 51. https://doi.org/10.5337/2013.205

Kebede, S. (2013). Groundwater in Ethiopia. In *Features, numbers and opportunities* (p. 283). Heidelberg: Springer. https://doi.org/10.1007/978-3-642-30391-3

Kværnø, S. H., Engebretsen, A., Barneveld, R., & Deelstra, J. (2016). Applying profile- and catchment-based mathematical models for evaluating the run-off from a Nordic catchment. *Journal of Hydrology and Hydromechanics*, *64*, 218–225. https://doi.org/10.1515/johh-2016-0022

Leiriao, S., He, X., Christiansen, L., Andesen, O. B., & Bauer-Gottwein, P. (2009). Calculation of the temporal gravity variation from spatially variable water storage change in soils and aquifers. *Journal of Hydrology*, *365*, 302–309. https://doi.org/10.1016/j.jhydrol.2008.11.040

Liu, B. M., Collick, A. S., Zeleke, G., Adgo, E., Easton, Z. M., & Steenhuis, T. S. (2008). Rainfall discharge relationships for a monsoonal climate in the Ethiopian highlands. *Hydrological Processes*, *22*, 1059–1067. https://doi.org/10.1002/hyp.7022

Mechal, A., Wagner, T., & Birk, S. (2015). Recharge variability and sensitivity to climate: The example of Gidabo River basin, main Ethiopian rift. *Journal of Hydrology: Regional Studies*, *4*, 644–660. https://doi.org/10.1016/j.ejrh.2015.09.001

Meinzer, O. E. (1923). *The occurrence of ground water in the United States with a discussion of principles*. (Water Supply Paper 489). U.S. Government Printing Office, Washington, DC. https://doi.org/10.3133/wsp489

Nikroo, L., Kompani-Zare, M., Sepaskhah, A. R., & Shamsi, S. R. F. (2010). Groundwater depth and elevation interpolation by kriging methods in Mohr Basin of Fars province in Iran. *Environmental Monitoring and Assessment*, *166*, 387–407. https://doi.org/10.1007/s10661-009-1010-x

Otoo, M., Lefore, N., Schmitter, P., Barron, J., & Gebregziabher, G., (2018). *Business model scenarios and suitability: Smallholder solar pump-based irrigation in Ethiopia. Agricultural Water Management—Making a Business Case for Smallholders*. (IWMI Research Report 172; 67 p.). International Water Management Institute (IWMI), Colombo, Sri Lanka. https://doi.org/10.5337/2018.207

Pavelic, P., Smakhtin, V., Favreau, G., & Villholth, K. G. (2012). Water-balance approach for assessing potential for smallholder groundwater irrigation in sub-Saharan Africa. *Water SA*, *38*, 399–406. https://doi.org/10.4314/wsa.v38i3.5

Pool, D., & Eychaner, J. (1995). Measurements of aquifer-storage change and specific yield using gravity surveys. *Groundwater*, *33*, 425–432. https://doi.org/10.1111/j.1745-6584.1995.tb00299.x

Schmitter, P., Kibret, K. S., Lefore, N., & Barron, J. (2018). Suitability mapping framework for solar photovoltaic pumps for smallholder farmers in sub-Saharan Africa. *Applied Geography*, *94*, 41–57. https://doi.org/10.1016/j.apgeog.2018.02.008

Sopocleous, M. A. (1991). Combining the soil water balance and water-level fluctuation methods to estimate natural groundwater storage: Practical aspects. *Journal of Hydrology*, *124*, 229–241.

Steenhuis, T. S., Jackson, C. D., Kung, S. K., & Brutaert, W. (1985). Measurement of groundwater storage on eastern Long Island, New York, USA. *Journal of Hydrology*, *79*, 145–169. https://doi.org/10.1016/0022-1694(85)90190-8

Steenhuis, T. S., & van der Molen, W. H. (1986). The ThornthwaiteMather procedure as a simple engineering method to predict recharge. *Journal of Hydrology*, *84*, 221–229. https://doi.org/10.1016/0022-1694(86)90124-1

Tebebu, T. Y., Steenhuis, T. S., Dagnew, D. C., Guzman, C. D., Bayabil, H. K., Zegeye, A. D., … Tilahun, S. A. (2015). Improving efficacy of landscape interventions in the (sub) humid Ethiopian highlands by improved understanding of runoff processes. *Frontiers in Earth Science*, *3*, 49. https://doi.org/10.3389/feart.2015.00049

Theis, C. V. (1935). *The relation between the lowering of the piezometric surface and the rate and duration of discharge of a well using ground water storage, Eos*. (Transaction of the American Geological Union 16), 368-350S US Department of the Interior, Geological Survey, Water Resources Division, Ground Water Branch. https://doi.org/10.1029/TR016i002p00519

Thornthwaite, C. W., & Mather, J. R. (1955). The water balance. *Publications in Climatology*, *8*(1–104), 1955.

Tilahun, S. A., Ayana, E. K., Guzman, C. D., Dagnew, D. C., Zegeye, A. D., Tebebu, T. Y., … Steenhuis, T. S. (2016). Revisiting storm runoff processes in the upper Blue Nile basin: The Debre Mawi watershed. *Catena*, *143*, 47–56. https://doi.org/10.1016/j.catena.2016.03.029

Tilahun, S. A., Guzman, C. D., Zegeye, A. D., Dagnew, C. D., Collick, A. S., Yitaferu, B., & Steenhuis, T. S. (2015). Distributed discharge and sediment concentration predictions in the sub-humid Ethiopian highlands: The Debre Mawi watershed. *Hydrological Processes*, *29*, 1817–1828. https://doi.org/10.1002/hyp.10298

Tilahun, S. A., Guzman, C. D., Zegeye, A. D., Engda, T. A., Collick, A. S., Rimmer, A., & Steenhuis, T. S. (2013). An efficient semi-distributed hillslope erosion model for the sub humid Ethiopian highlands. *Hydrology and Earth System Sciences*, *17*, 1051–1063. https://doi.org/10.5194/hess-17-1051-2013

Tilman, D., Cassman, K. G., Matson, P. A., Naylor, R., & Polasky, S. (2002). Agricultural sustainability and intensive production practices. *Nature*, *418*, 671–676. https://doi.org/10.1038/nature01014

Tucker, J., & Yirgu, L. (2011). *Water in food security assessment and drought early warning: Experiences from sub-Saharan Africa with a special focus on Ethiopia*. (RiPPLE Working Paper 21). Addis Ababa: RiPPLE.

Veihmeyer, F., & Hendrckson, A. (1931). The moisture equivalent as a measure of the field capacity of soils. *Soil Science*, *32*, 181–194. https://doi.org/10.1097/00010694-193109000-00003

Vörösmarty, C. J., Ellen, M. D., Green, P. A., & Revenga, C. (2005). Geospatial indicators of emerging water stress: An application to Africa. *Ambio*, *34*, 230–236. https://doi.org/10.1579/0044-7447-34.3.230

Walker, D., Parkin, G., Schmitter, P., Gowing, J., Tilahun, S. A., Haile, A. T., & Yimam, A. Y. (2018). Insights from a multi-method recharge estimation comparison study. *Groundwater*, *57*, 245–258. https://doi.org/10.1111/gwat.12801

Walraevens, K., Tewolde, T. G., Amare, K., Hussein, A., Berhane, G., Baert, R., … Deckers, J. (2015). Water balance components for sustainability assessment of groundwater-dependent agriculture: Example of the Mendae plain (Tigray, Ethiopia). *Land Degradation & Development*, *26*, 725–736. https://doi.org/10.1002/ldr.2377

Walraevens, K., Vandecasteele, I., Martens, K., Nyssen, J., Moeyersons, J., Gebreyohannes, T., … Van Camp, M. (2009). Groundwater storage and flow in a small mountain catchment in northern Ethiopia. *Hydrological Sciences Journal*, *54*, 739–753. https://doi.org/10.1623/hysj.54.4.739

Walton, W. C. (1970). *Groundwater resource evaluation* (p. 664). New York: McGraw-Hill.

Worqlul, A. W., Collick, A. S., Rossiter, D. G., Langan, S., & Steenhuis, T. S. (2015). Assessment of surface water irrigation potential in the Ethiopian highlands: The Lake Tana Basin. *Catena*, *129*, 76–85. https://doi.org/10.1016/j.catena.2015.02.020

Xie, H., You, L., Wielgosz, B., & Ringler, C. (2014). Estimating the potential for expanding smallholder irrigation in sub-Saharan Africa. *Agricultural Water Management*, *131*, 183–193. https://doi.org/10.1016/j.agwat.2013.08.011

You, L., Ringler, C., Wood-Sichra, U., Robertson, R., Wood, S., Zhu, T., … Sun, Y. (2011). What is the irrigation potential for Africa? A combined biophysical and socioeconomic approach. *Food Policy*, *36*, 770–782. https://doi.org/10.1016/j.foodpol.2011.09.001

SUPPORTING INFORMATION

Additional supporting information may be found online in the Supporting Information section at the end of this article.

How to cite this article: Tilahun SA, Yilak DL, Schmitter P, et al. Establishing irrigation potential of a hillside aquifer in the African highlands. *Hydrological Processes*. 2020;34:1741–1753. https://doi.org/10.1002/hyp.13659